Available online at www.sciencedirect.com
SCIENCE DIRECT®
International Journal of Pharmaceutics 254 (2003) 211–222
international journal of pharmaceutics
www.elsevier.com/locate/ijpharm

Release mechanism of insulin encapsulated in trehalose ester derivative microparticles delivered via inhalation

Iain G. Davidson, Eric J. Langner, Steven V. Plowman, Julian A. Blair*

Elan Drug Delivery, 1 Mere Way, Ruddington, Nottinghamshire NG11 6JS, UK

Received 20 August 2002; received in revised form 17 December 2002; accepted 7 January 2003

Abstract

The aim of this study was to evaluate properties of amorphous oligosaccharide ester derivative (OED) microparticles in order to determine drug release mechanisms in the lung. Trehalose OEDs with a wide range of properties were synthesised using conventional methods. The interaction of spray dried amorphous microparticles (2–3 μm) with water was investigated using attenuated total reflectance Fourier transform infra-red spectroscopy (ATR-FTIR) and dynamic vapour sorption (DVS). The in vivo performance of insulin/OED microparticles was assessed using a modified Higuchi kinetic model. A modified Hansen solvent parameter approach was used to analyse the interactions with water and in vivo trends. In water or high humidity, OED powders absorb water, lose relaxation energy and crystallise. The delay of the onset of crystallisation depends on the OED and the amount of water present. Crystallisation follows first order Arrhenius kinetics and release of insulin from OED microparticles closely matches the degree of crystallisation. The induction period depends on dispersive interactions between the OED and water while crystallisation is governed by polarity and hydrogen bonding. Drug release from OED microparticles is, therefore, controlled by crystallisation of the matrix on contact with water. The pulmonary environment was found to resemble one of high humidity rather than a liquid medium.

Keywords: Microparticle; Controlled release; Inhalation

1. Introduction

Control over drug release kinetics is of strategic importance in modern therapeutic drug delivery. Controlled release technologies can be tailored to bring a number of benefits, including increased pharmacological efficacy, extended duration of action, greater flexibility of administrative route and improved targeting of specific disease sites (Ron and Langer, 1992).

Bioerodible controlled release technologies based on, for example, the polyesters, are costly to synthesise, can be physically unstable and are subject to the build-up of acidic metabolites in the matrix prior to drug release. In addition to these limitations, emulsification is often used to prepare polymeric microparticle systems and can result in poor drug encapsulation and stability (Cleland, 1997; Roskos and Maskiewicz, 1997). Oligosaccharide ester derivatives (OEDs) were designed to help overcome these problems (Gribbon et al., 1996).

Many carbohydrates form relatively stable amorphous phases, for instance by rapid cooling from the melt. These amorphous solids (glasses) can be convenient matrices for hosting, stabilisation and delivery of biologically active molecules (Gribbon et al., 1996). Generally, carbohydrates are highly susceptible to

* Corresponding author. Tel.: +44-115-974-7474; fax +44-115-974-8494.
E-mail address: blairj@quadrant.co.uk (J.A. Blair).

0378-5173/03/$ – see front matter
doi:10.1016/S0378-5173(03)00035-8

attack by water, in either the gaseous or liquid phase, which has a plasticising effect, leading rapidly to crystallisation or dissolution of the matrix. By selectively replacing hydroxyl groups on disaccharide molecules with more lipophilic functionalities, it is possible to reduce the extent and rate of this interaction with water and, therefore, to regulate this plasticising effect and consequent crystallisation (Gribbon et al., 1996; Hatley and Blair, 1999).

Insulin is currently given by injection for the treatment of diabetes; however, delivery via the lung is receiving much interest within the pharmaceutical industry. OEDs have been formulated with insulin as dry microparticles having aerodynamic properties necessary for administration to the deep lung (Blair et al., 2002). This work sets out to establish important physicochemical properties of OEDs and their impact on the release mechanism of insulin from these matrices.

2. Materials and methods

2.1. Materials

Unless otherwise stated all chemicals were of standard laboratory grade. All materials used in the synthesis of OEDs were obtained from Fisher Chemicals (Loughborough, UK). Trehalose octaacetate was obtained from Sigma (Poole, UK) and trehalose dihydrate was obtained from Hayashibara (Japan). Reference compounds used in the determination of OED lipophilicity were of analytical grade and obtained from Aldrich (Gillingham, UK) and recombinant human insulin was obtained from a commercial supplier.

2.2. Synthesis of OEDs

Simple alkyl esters of trehalose, where the ester groups are all the same, were prepared using known methods (Whistler and BeMiller, 1972). Mixed esters were synthesised either via ditrityl trehalose (Bredereck, 1930) or dibenzylidene trehalose (Baer and Radatus, 1984). The trityl groups were most readily removed by the method of Ding et al. (1997) using $FeCl_3$, benzylidene deprotection was cleanly achieved with aqueous TFA (Baer and Abbas, 1979). Esterification of the resulting unprotected compounds was carried out either using acid chlorides in pyridine or by a dicyclohexyl carbodiimide (DCC)-mediated coupling (Scriven, 1983). ^{1}H NMR were measured using a Bruker DRX-500MHz Spectrometer.

2.2.1. 6,6′-Diisobutyroyl-2,3,4:2′,3′,4′-hexaacetyl trehalose (TR122)

TR122 was prepared by the reaction of isobutyroyl chloride with hexaacetyl trehalose in dry pyridine. Recrystallisation from 3:1 methanol/water gave the product (84%) as a white crystalline solid; m.p. 89–92 °C; δ ($CDCl_3$) 5.24 (2H, d, H-1,1′), 5.02 (2H, dd, H-2,2′), 5.45 (2H, t, H-3,3′), 5.03 (2H, t, H-4,4′), 3.96–4.08 (4H, m, H-5,5′,6,6′), 4.20 (2H, cm, H-6,6′), 2.55 (2H, sept, 2C–H), 2.06 (6H, s, $2CH_3$), 2.02 (6H, s, $2CH_3$), 2.00 (6H, s, $2CH_3$), 1.15, 1.14, 1.12, 1.11 (12H, s, $4CH_3$).

2.2.2. 6:6′-Dicyclohexanoyl-2,3,4:2′,3′,4′-hexaacetyl trehalose (TR148)

TR148 was prepared by the DCC-mediated reaction of cyclohexanoic acid with hexaacetyl trehalose in acetonitrile. Recrystallisation from IMS gave the product (73%) as a white crystalline solid; m.p. 154 °C; δ ($CDCl_3$) 5.46 (2H, t, H-3,3′), 5.24 (2H, d, H-1,1′), 5.04 (2H, t, H-4,4′), 5.04 (2H, dd, H-2,2′), 4.21 (2H, dd, H-6a,a′), 4.05 (2H, cm, H-5,5′), 3.98 (2H, d, 6b,b′), 2.30 (2H, cm, cycloCH), 2.06 (6H, s, $2AcCH_3$), 2.02 (6H, s, $2AcCH_3$), 2.00 (6H, s, $2AcCH_3$), 1.87 (4H, cm, cycloCH), 1.74 (4H, cm, cycloCH), 1.63 (2H, cm, cycloCH), 1.38 (4H, cm, cycloCH), 1.24 (6H, cm, cycloCH).

2.2.3. 6:6′-bis(β-Tetraacetyl glucuronyl)hexaacetyl trehalose (TR153)

TR153 was prepared by the DCC-mediated reaction of β-tetraacetyl glucuronic acid with hexaacetyl trehalose. Recrystallisation from ethanol gives the product (71%) as a white powder; m.p. 156 °C; δ ($CDCl_3$) 5.76 (2H, d, G-1), 5.46 (2H, t, T-3), 5.25 (6H, cms, T-1, G-3,4), 5.18 (2H, t, G-2), 5.02 (2H, dd, T-2), 4.92 (2H, t, T-4), 4.25 (2H, d, G-5), 4.14 (2H, d, T-6a), 4.06 (2H, dd, T-6b), 3.99 (2H, m, T-5), 2.08 (6H, s, $2CH_3$), 2.06 (6H, s, $2CH_3$), 2.01 (24H, 3s, $8CH_3$), 1.98 (6H, s, $2CH_3$). T = trehalose proton; G = glucuronyl proton.

2.2.4. 6:6′-bis(β-Tetraacetyl glucuronyl)-2,3:2′,3′-tetraisobutyroyl-4:4′-diacetyl trehalose (TR155)

TR155 was prepared as earlier from tetraisobutyroyl trehalose. Esterification gives only the 6:6′-disubstituted product due to steric hinderance. Subsequent acetylation of the remaining free hydroxyl groups and recrystallisation from methylated spirits gives 6:6′-bis(β-tetraacetyl glucuronyl)-2,3:2′,3′-tetraisobutyroyl-4:4′-diacetyl trehalose (75%) as an amorphous white powder. δ ($CDCl_3$) 5.76 (2H, d, G-1), 5.50 (2H, t, T-3), 5.33 (2H, d, T-1), 5.26 (4H, m, G-3,4), 5.18 (2H, t, G-2), 4.98 (2H, dd, T-2), 4.96 (2H, t, T-4), 4.24 (2H, d, G-5), 4.09 (2H, d, T-6a), 4.01 (2H, dd, T-6b), 3.86 (2H, m, T-5), 2.54 (2H, sept, CH), 2.48 (2H, sept, CH), 2.08 (6H, s, $2CH_3$), 2.00 (6H, s, $2CH_3$), 1.99 (24H, 3s, $8CH_3$), 1.97 (6H, s, $2CH_3$), 1.95 (6H, s, $2CH_3$), 1.14 (6H, s, $2CH_3$), 1.13 (6H, s, $2CH_3$), 1.10,1.09, 1.08, 1.07 ($4 \times 3H$, 4s, $4CH_3$).

2.3. Materials characterisation

Thermal analysis was carried out using a Perkin-Elmer DSC7 Differential Scanning Calorimeter (DSC). Glass transition temperatures were determined by heating a crystalline sample (~10 mg) in a 40 μl aluminium pan with a pierced lid to 20 °C above T_m, cooling to 20 °C below the glass transition temperature (T_g) and then reheating to above T_m all at 10 °C min^{-1}. Pyris 1 software was used to calculate T_g as $1/2\Delta C_p$ extrapolated and T_m as the onset of the melt endotherm.

Octanol–water partition coefficients ($\log P_{ow}$) were determined using an HPLC method (Official Journal of the European Communities, 1992a). The retention times of OEDs and reference compounds of known $\log P_{ow}$ were measured on a Phenomenex Jupiter (C18 250 mm × 4.6 mm, 5 μm) column with 75:25 acetonitrile/water as mobile phase. Detection was by UV absorption at 209 nm. The lipophilicity of test compounds was calculated from a linear correlation of $\log P_{ow}$ and capacity factor (k) for the reference materials.

The solubilities of OEDs were measured at 25 °C in a range of solvents using a shake flask method (Official Journal of the European Communities, 1992b). An excess of crystalline solid was equilibrated with solvent and the supernatants analysed by HPLC against standard solutions of known concentration. This process was repeated until the solutions had reached equilibrium.

2.4. Preparation and characterisation of microparticles

OED microparticles were prepared by spray drying a 5% w/v dichloromethane solution using a Buchi 191 Mini Spray Dryer (Buchi Labortechnik, Switzerland) with a two fluid nozzle. The inlet temperature was 60 °C, atomisation pressure 2 bar and feed rate 4 ml min^{-1}. The particles were collected from the cyclone and collection jar and stored in sealed vials.

Methods for the preparation of amorphous OED microparticles containing insulin are reported elsewhere (Blair et al., 2002), and consist of spray drying a feed solution containing insulin (10% w/w), dipalmitoylphosphatidylglycerol (DPPG) (2% w/w) and OED (88% w/w) in a solution of DMSO and acetone (50/50 v/v) using a Buchi 191 Mini Dryer maintaining the outlet temperature below 90 °C.

The mass median aerodynamic diameters (MMADs) of the particles produced were determined using an Amherst API Aerosizer (TSI Amherst, USA). Morphology of the powders was determined by scanning electron microscopy (SEM). Samples (2–5 mg) were placed on an aluminium stub and sputter coated with 10–20 nm of gold before being viewed using a Philips XL30 Field Emission SEM operated at 15 kV.

2.5. Interaction of OED microparticles with water

The interactions with water and amorphous stability were investigated using attenuated total reflectance Fourier transform infra-red spectroscopy (ATR-FTIR). The spectra used in this study were acquired on a Perkin-Elmer Spectrum GX Spectrometer fitted with a Specac Golden Gate diamond ATR accessory. Sixteen co-added scans were used for each spectrum between 6000 and 1000 cm^{-1}. The resolution was 4 cm^{-1}. The spectra were acquired in transmission and normalised to 1.5 absorbance units using Perkin-Elmer Spectrum version 3.02. A new background spectrum was recorded prior to each sample spectrum. All subsequent processing was performed in MATLAB (MATLAB, 2001).

An atmosphere of 92% RH at 37 °C was generated using saturated solutions of ammonium dihydrogen-

phosphate in 200 ml glass bottles. The OED powders were held in the headspace in baskets and sampled at timed intervals. Interactions with liquid water were investigated by immersing the formulations in water at temperatures over the range 4–60 °C. Wet samples were filtered under vacuum for 2 min prior to presentation on the ATR bridge. The degree of crystallinity was determined by measurement of the absorbance bands at, e.g. 1120 cm^{-1} for TR153 and 1143 cm^{-1} for TR101. These bands were chosen from a number of alternatives due to their relative freedom from competing absorbancies. The crystalline content was determined relative to equivalent formulations, which were dispersed in water at 37 °C for 12 h. These crystalline standards were analysed for any amorphous content by DSC.

Insulin content was similarly determined by ATR-FTIR using the amide 2 region from 1530 to 1560 cm^{-1}. The release was determined relative to the spectrum at time 0.

Adsorption and desorption isotherms were determined by dynamic vapour sorption (DVS) using a DVS 1000 Moisture Sorption Analyser (Surface Measurement Systems Ltd., UK) with DVS-Win software. The powder (20 mg) was placed in the instrument and the humidity was ramped from 0 to 95% RH in 5% RH steps at 25 °C. Brunauer–Emmit–Teller (BET) treatment of the data allowed the calculation of the weight of the absorbed monolayer of water (Webb and Orr, 1997). As water strongly interacts with amorphous OED particles, the monolayer formed actually represents a hydration surface which is much larger than the true surface area (Zhang and Zografi, 2000). The true surface areas of the microparticles were determined by nitrogen adsorption using a Coulter SA 3100 Surface Analyser.

2.6. Pharmacokinetic study of insulin/OED microparticles

OED powders were administered to the lungs of rats using methods previously described (Blair et al., 2002). Formulations of pure spray dried insulin (11 U kg^{-1}) or insulin/OED formulation (56 U kg^{-1}), with similar aerosol properties, were administered to rats ($n = 12$) using a PennCentury Dry Powder Delivery Device. Bioavailability and absorption kinetics were assessed by monitoring plasma insulin levels over time. Blood samples were taken at set time points post-dosing and assayed for human insulin using a radio immunoassay. This method was used to distinguish between the administered human insulin and endogenous rat insulin and to assess the viability of the administered insulin. Plasma insulin concentration/time profiles were processed using an approach based on a modified Higuchi kinetic model (Higuchi, 1963). All procedures carried out on live animals as part of this study were subject to the provisions of United Kingdom law, in particular the Animals (Scientific Procedures) Act, 1986.

Table 1
Structure and properties of selected OEDs

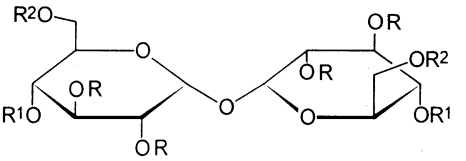

Code	R	R^1	R^2	T_g (°C)	T_m (°C)	M_w	log P
TR101	Ac	Ac	Ac	55	135	678	0.97
TR122	Ac	Ac	iBu	42	92–95	734	2.11
TR148	Ac	Ac	cHex	58	154	814	4.64
TR153	Ac	Ac	β-TAG	110	154	1282	2.92
TR155	iBu	Ac	β-TAG	92	–	1394	4.46

Ac is acetyl, iBu is isobutyroyl, cHex is cyclohexanoyl and β-TAG is β-tetraacetyl glucuronyl.

3. Results

3.1. Physicochemical characterisation

The structures of some selected OEDs and their physical properties are presented in Table 1. Spray dried particles of OEDs had MMAD of 2–3 μm and were smooth spheres. Insulin/OED formulations were also 2–3 μm in diameter and were found to be dimpled spheres (Fig. 1).

3.2. Interaction of OED microparticles with water

Amorphous TR101 microparticles were immersed in water at 37 °C and the rate of crystallisation was determined by the growth of a peak at 1143 cm^{-1} (Fig. 2A). Crystallisation of TR153 was similarly fol-

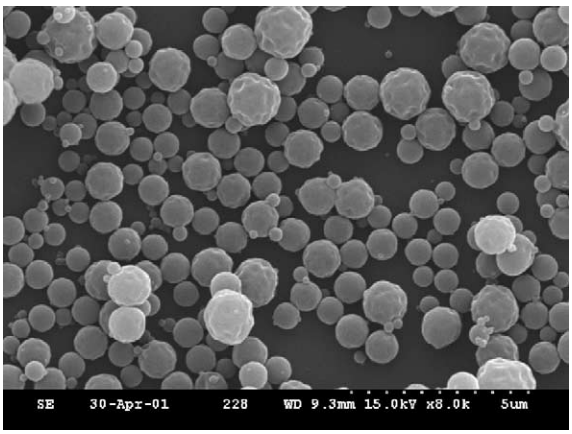

Fig. 1. SEM of spray dried insulin/OED microparticles.

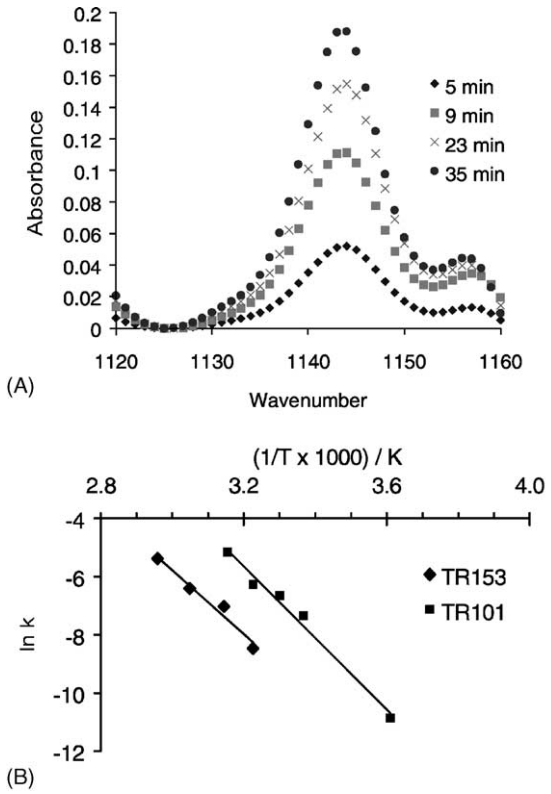

Fig. 2. FTIR data. (A) Increase in crystalline content with time in water at 37 °C is illustrated for TR101. (B) Arrhenius plots for the crystallisation of TR153 and TR101.

lowed at 1120 cm^{-1}. TR155 showed no crystallinity in any of the experiments.

The process of crystallisation was modelled using the empirical logistic equation (Cerny et al., 1981) in a modified form (ORIGIN, 1995) (Eq. (1)), where P is the value at time t, I is the infinity value, e the order of the curve and $t_{1/2}$ is the half-life.

$$P = -\frac{I}{1 + (t/t_{1/2})^e} + I \quad (1)$$

This equation is widely used for the fitting of sigmoidal and, when $e = 1$, exponential data (Cerny et al., 1981). For TR153, a delay between the immersion of the particles in water and the onset of crystallisation of around 20 min was observed. This is termed the induction period. This induction period was not included in the curve fitting process. Half-lives for the crystallisation of 6 min for TR101 and 55 min for TR153 were obtained from which were calculated first order rate constants of 1.93×10^{-3} s^{-1} for TR101 and 2.10×10^{-4} s^{-1} for TR153.

A plot of predicted against actual values was used to determine the accuracy of the curve fitting. In both cases R^2 was greater than 0.98.

The Arrhenius behaviour of the crystallisation process for both TR101 and TR153 was demonstrated by performing the experiment over a range of temperatures (Fig. 2B). The activation energies were found to be similar in both cases—91 kJ mol^{-1} for TR153 and 101 kJ mol^{-1} for TR101. Release of insulin from TR153 was shown to closely follow the crystallisation, with a plot of degree of crystallinity against percentage insulin release giving a correlation coefficient of 0.99.

The induction periods prior to crystallisation and the half-lives at 92% RH and 37 °C are reported in Table 2. Again, TR155 showed no crystallinity in any of the experiments.

When spray dried amorphous OED microparticles were investigated by DVS, significant amounts of water were absorbed (Table 2). The exception to this was TR148 which only absorbed 0.4% by weight of water and gave a type 3 adsorption isotherm so that BET analysis was not possible (Webb and Orr, 1997). The surface areas calculated from nitrogen absorption (Table 2) were all 2–3 m^2 g^{-1} as expected for near spherical particles of around 2 μm diameter.

Table 2
Surface analysis and crystallisation of OED microparticles

OED	True surface area ($m^2\,g^{-1}$)	W_m ($g\,100\,g^{-1}$)[a]	Induction period (h)	Crystallisation half-life (h)
TR101	2.08	0.68	1.2	0.25
TR148	–	–	8.3	28
TR153	2.20	0.98	67	>2000
TR155	3.32	0.62	>100	–

[a] W_m is the mass of water adsorbed at monolayer coverage. The crystallisation conditions were 92% relative humidity at 37 °C.

3.3. Determination of solubility and related parameters

The solubilities of OEDs in common solvents are listed in Table 3. The solubility of TR148 was not determined. These data were used to derive solubility parameters (Table 3) which were used to develop models for in vitro and in vivo trends in amorphous stability and drug release, respectively. A new set of solute specific parameters (d, p, h, I) were derived during the course of this work as regression coefficients in a simple multilinear relationship (Eq. (2)) to correlate solvent parameters of common solvents (Archer, 1992) with logarithm of OED solubility ($g\,l^{-1}$).

$$\log S_{ij} = D_j d_i + P_j p_i + H_j h_i + I_i \quad (2)$$

where S is the solubility of solute i in solvent j, the regression coefficients, d, p, h, I, represent the solute specific dispersion, polar, hydrogen bonding and solubility offset parameters of solute i. Terms D, P, and H are the Hansen parameter set of solvent j. Hansen parameters of OEDs were derived separately using a paired solvent approach (Hansen and Anderson, 1988).

Experimentally derived solubility parameters were modelled (Table 3) using empirical relationships (Eq. (3)) based on lipophilicity and molecular weight contributions,

$$Y_{xi} = a(P_i + b)^c + d(M_i + e)^f + g \quad (3)$$

where Y is the xth solubility parameter of compound i, P is lipophilicity ($\log P_{ow}$) and M is molecular weight of the ith compound and a, b, c, d, e, f and g are

Table 3
Interaction of OEDs with solvents

	OED solubility ($g\,l^{-1}$) at 25 °C			
	TR101	TR122	TR153	TR155
Solvent				
Acetone	424	571	269	765
Dichloromethane	609	989	316	529
Dimethylsulphoxide	321	262	300	595
Ethanol	2.34	31.3	0.2	32
Ethyl acetate	177	231	515	ND
Water	0.056	0.013	0.010	0.003
OED solvent and solute specific parameters				
Hansen dispersion (D) ($MPa^{-0.5}$)	17.4	16.8	17.1	16.7
Hansen polarity (P) ($MPa^{-0.5}$)	11.9	10.4	11.1	10.8
Hansen hydrogen bonding (H) ($MPa^{-0.5}$)	8.5	11.4	8.8	11.3
Solute dispersion (d) ($g\,l^{-1}\,MPa^{-0.5}$)	0.10	0.06	−0.11	−0.08
Solute polarity (p) ($g\,l^{-1}\,MPa^{-0.5}$)	0.05	0.00	0.22	0.10
Solute hydrogen bonding (h) ($g\,l^{-1}\,MPa^{-0.5}$)	−0.12	−0.13	−0.19	−0.17
Correlation intercept (I) ($g\,l^{-1}\,MPa^{-0.5}$)	1.10	2.65	3.45	4.47
Correlation coefficient (R^2)	0.968	0.985	0.800	0.964
Number of degrees of freedom (n)	2	2	8	6
F-statistic	20.2	43.9	10.7	53.1

Table 4
Plasma insulin concentrations

Time (min)	Average plasma insulin concentration (uU ml^{-1})					
	TR153		TR101		TR148	
	Concentration (uU ml^{-1} plasma)	Standard deviation ($n = 12$)	Concentration (uU ml^{-1} plasma)	Standard deviation ($n = 12$)	Concentration (uU ml^{-1} plasma)	Standard deviation ($n = 12$)
0	0		0		0	
5	1270	360	5940	3350	3480	1560
20	4660	2050	11200	2020	11600	4190
60	630	430	8100	3650	12300	5350
120	290	60	1440	1350	5620	1820
240	110	20	320	40	1020	280
480	40	10	70	20	70	20
600	70	50	60	50	50	10
720	50	20	40	10	40	10
1440	30	10	10	10	10	10

constants common to the whole series. Empirical relationships were established by iterating the value of each constant and correlating experimentally derived and modelled parameters until F-statistic and R^2 values were maximised. In each case F was greater than 100 and R^2 greater than 0.97. These relationships were used to estimate the solubility parameters of OEDs outside the dataset, including formulations, where averaged values of lipophilicity and molecular weight were used.

Solubility parameter models that describe trends in the induction period and crystallisation half-lives of experiments carried out at 92% humidity and 37 °C are illustrated in Fig. 3A and B, respectively. A correlation was found between the sum of the internal polar and hydrogen bonding parameters ($P_i p_i + H_i h_i$) and the DVS hydration surface as measured by W_m (Fig. 3C).

3.4. Determination of in vivo release mechanism

The cumulative insulin plasma concentrations determined at timed intervals after intra-tracheal administration of OED formulations to the lungs of rats are reported in Table 4. These data were processed using

Table 5
Higuchi analysis of plasma insulin concentrations

Time (min)	Cumulative plasma insulin concentration (μU ml^{-1})					
	TR153		TR101		TR148	
	$i = 1$	$i = 2$	$i = 1$	$i = 2$	$i = 1$	$i = 2$
0	0		0		0	
5	1270		5940		3480	
20	5930		17100		15100	
60	6570		25200		27400	
120	6870	6870	26700	26700	33000	33000
240		6980		27000		34100
480		7020		27100		34100
600		7090		27100		34200
720		7140		27200		34200
1440		7170		27200		34200
Mean slope—m_i	76	0.184	295	0.132	355	0.360
Mean intercept—c_i	1680	6940	5300	27000	3410	33800

When $i = 1$ the slopes and intercepts were evaluated from 0 to 60 min and from 0 to 120 min. When $i = 2$ the slopes and intercepts were evaluated from 120 to 1440 min and from 240 to 1440 min.

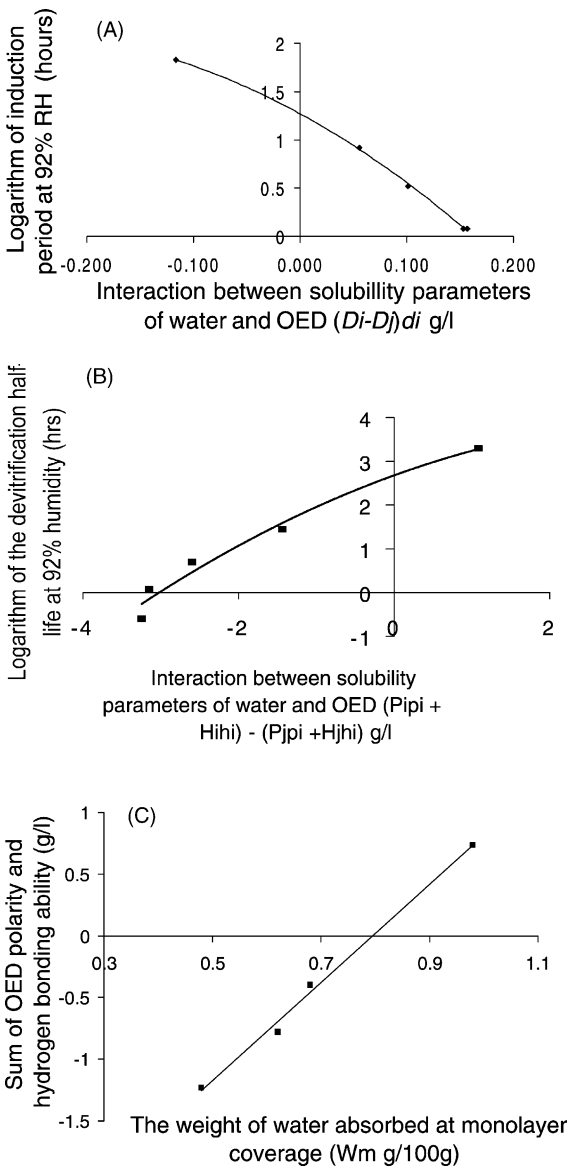

Fig. 3. Relationships between solubility parameters and interaction with water. (A) The in vitro induction period is related to the difference in dispersivity between OEDs and water. (B) The rate of in vitro crystallisation is related to the size of non-occupied hydration surface. (C) The formation of a hydration surface is related to the sum of polarity and hydrogen bonding.

a modified Higuchi kinetic model (Higuchi, 1963), which gave two slopes and two intercepts per experiment (Eq. (4)), where A is the cumulative insulin plasma concentration (μU) raised to a power n (the degree of curvature) at time t (min) raised to a power (p), m is the gradient and c is the intercept for the ith relationship.

$$\sum_{t=0}^{t=t} A^n = m_i t^p + c_i \tag{4}$$

For the unmodified Higuchi kinetic model $n = 1$ and $p = 0.5$. However, in this study n and $p = 1$ because relationships between cumulative plasma concentration and time were intrinsically composed of two stages, a fast initial phase ($i = 1$) and a much slower secondary phase ($i = 2$) which were well resolved. Characteristic values for m and c in this study are given in Table 5.

The solubility parameters (Table 3) were used in the construction of models relating the onset of the release of insulin to the loss of relaxation energy (Fig. 4A) and the secondary insulin release to the solubility of the matrix in water (Fig. 4B).

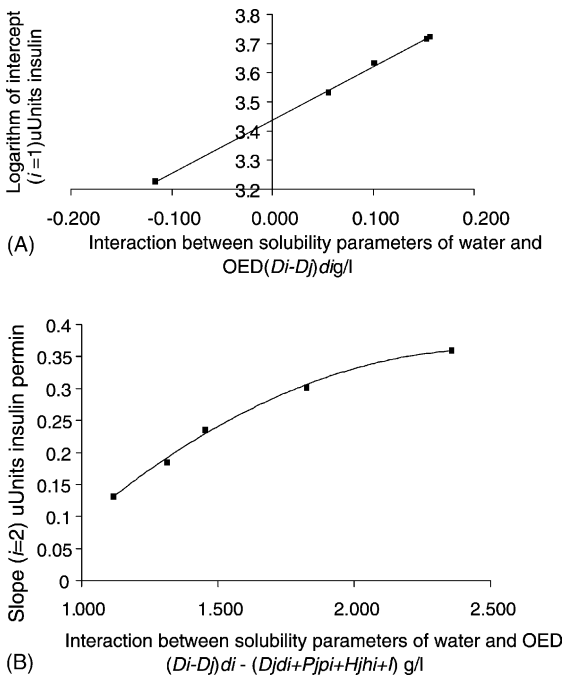

Fig. 4. Correlation of solubility and Higuchi parameters for in vivo study. (A) The onset of insulin release is related to the loss of relaxation energy from the matrix. (B) The rate of insulin release is related to the solubility of the matrix in water.

4. Discussion

For an OED to be suitable as a matrix for formulation and controlled delivery of an active substance, the T_g must be well above any storage temperature to prevent plasticisation and aggregation of the particles. In addition the material must be sufficiently lipophilic to prevent rapid dissolution in aqueous environments while allowing in vivo metabolism and preventing bioaccumulation. Therefore, materials were targeted that had a minimum T_g of 55 °C, preferably greater than 70 °C, and a $\log P_{ow}$ of between 1 and 4.5.

Trehalose was chosen as the template for synthesis of OEDs as it is a symmetrical non-reducing disaccharide and so a variety of functionality is readily available through standard protecting group strategies without the complication of anomeric mixtures.

Spray dried microparticles of trehalose octaacetate rapidly recrystallise when subjected to high humidity or dispersed in water. Therefore, the need for materials with a more stable amorphous form—higher T_g, $\log P_{ow}$—was identified. The inclusion of straight chain esters—e.g. propanoyl, *n*-butanoyl—increased $\log P_{ow}$ with increasing chain length while rapidly decreasing T_g. Branched esters—e.g. isobutyroyl, *t*-butylacetyl—reduced T_g less than the analogous straight chain esters but many of these compounds were exceptionally lipophilic ($\log P_{ow} > 6.3$). Only the inclusion of *t*-butanoyl (pivaloyl) esters increased the T_g beyond that of the octaacetate. Cyclohexanoate esters gave higher T_g than much smaller straight chain esters, presumably due to the structural rigidity of the alkyl rings.

Using higher saccharides, e.g. maltotriose, as the parent compounds gave an increase in T_g over the corresponding disaccharides without greatly increasing lipophilicity. However, synthesis of oligosaccharides is complex and so an alternative strategy was devised. Using glucuronic acid derivatives to esterify trehalose at the 6-positions gave compounds containing four saccharide units. It was found that such compounds had high T_g while having $\log P_{ow}$ within the desired range. It is possible that conformational studies on both crystalline and amorphous forms of these materials may provide an understanding of their properties.

Although OEDs are poorly water soluble compounds, once solubilised they are readily hydrolysed at physiological pH—the hydrolytic half-life of TR101 at pH 7, 20 °C is 7.2 h. It should be noted that the presence of ester groups in the OED structures may facilitate metabolism as each hydrolysis yields progressively more water soluble compounds.

When dispersed in water, OED microparticles exhibit a range of behaviour. TR101, TR148 and TR153 all crystallise, TR122 quickly plasticises while TR155 remains completely amorphous. TR153 exhibits a delay of around 20 min before crystallisation begins. This induction period is thought to represent the loss of relaxation energy caused by the interaction with water and so was not included in the calculation of the rate of crystallisation. The crystallisation of the OED microparticles was assumed to be a pseudo first order process. This assumption was supported by the linear Arrhenius plots obtained from the calculated data.

Although TR155 does not crystallise in this experiment, it may be that the induction period for this material is exceptionally long. Although the reluctance of TR155 to crystallise is not fully understood, it may be due either the high viscosity of the system preventing molecular mobility or to the isobutyrate groups on the trehalose ring presenting a steric barrier to achieving the conformation required for crystallisation.

DVS experiments show that although the OEDs are lipophilic, as amorphous particulates with a high surface to volume ratio, they show a rapid and significant uptake of water. When the crystallisation of OED microparticles was followed at 92% RH, it was seen that even TR101 has a measurable induction period before the onset of crystallisation and that TR153 crystallises only very slowly (Table 2). Therefore, the rate of crystallisation of OEDs is greatly influenced by the amount of water present.

Measured lipophilicity (Table 1) and crystallisation experiments (Table 2) are not consistent with the results of DVS analysis (Table 2). Materials of low $\log P_{ow}$ and low amorphous stability may be expected to have greater interaction with water than high $\log P_{ow}$ and stable amorphous materials which should be indicated by higher W_m values. However, TR101 ($W_m = 0.68$, $\log P_{ow} = 0.97$) has a smaller hydration surface than the more lipophilic TR153 ($W_m = 0.98$, $\log P_{ow} = 2.92$) and is very similar to TR155 ($W_m = 0.62$, $\log P_{ow} = 4.46$). This can be rationalised by considering the ability of OEDs to form hydration surfaces from a polarity and hydrogen bonding perspective. Fig. 3C shows that as the sum of

internal polar and hydrogen bonding ability increases so does the tendency to form larger hydration surfaces. This suggests that polar and hydrogen bonding forces in OEDs overcome the tendency of lipophilic OED particles to repel water.

Solvent parameter modelling shows that the induction period prior to crystallisation depends on the interaction between solvent and solute dispersivity (Fig. 3A). After loss of this relaxation energy ($D_i d_i - D_j d_i$) the crystallisation process (Fig. 3B) was found to depend on the difference between the size of the hydration surface ($P_i p_i + H_i h_i$)—equivalent to W_m (Fig. 3C)—and the ease with which water molecules bind to it ($P_j p_i + H_j h_i$). If this were the case, we would expect an increase in the rate of crystallisation as coverage of the hydration surface increases indicated by ($P_i p_i + H_i h_i$)−($P_j p_i + H_j h_i$). The model (Fig. 3C) appears to fit the observed trend in data.

In summary, the crystallisation process at 92% humidity and 37 °C appears controlled by an initial dispersive interaction between OED and water molecules which lowers surface energy and which facilitates the formation of polar and hydrogen bonds between interacting molecules on the hydration surface. The crystallisation process usually results in expulsion of water molecules unless hydrates are formed. Our experience indicates hydrates are not usually formed, so expelled water is free to 'catalyse' further crystallisation. A 'catalytic' role for water agrees with the observed first order kinetics of the crystallisation process.

OEDs have been spray dried to form microparticles with a wide range of drugs, e.g. diltiazem (Ryan et al., 2000) or cyclosporin (Blair et al., 2000), as solid solutions. Peptides and proteins, such as leuprolide (Alcock et al., 2002), can be encapsulated in OED microparticles using hydrophobic ion pairing. Formulation with insulin (Blair et al., 2002) gives a suspension of the active within the OED matrix. Insulin was chosen as a model for this work for two reasons. Firstly, there is a growing interest throughout the pharmaceutical industry in the delivery of peptides to the lungs which would otherwise be given by injection and secondly, it does not interact directly with the OED matrix so allowing an independent study of the materials.

FTIR studies showed that the release of insulin from TR153 in vitro closely followed the crystallisation of the matrix, including the initial induction period (Fig. 5). This demonstrated that the encapsulated insulin was only released as the microparticles crystallise. The fact that TR155 neither crystallises nor releases insulin in this experiment supports this conclusion.

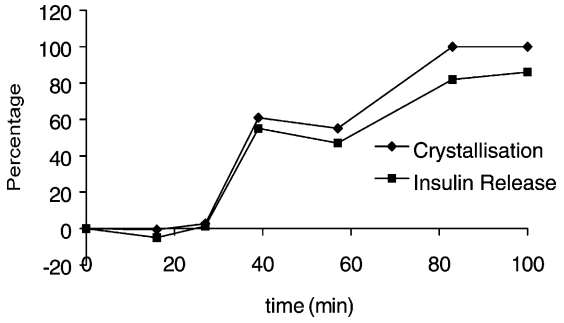

Fig. 5. Comparison of release of insulin with crystallisation of TR153.

Higuchi analysis of the in vivo data allows the cumulative insulin plasma concentration curves to be modelled as the sum of two straight lines representing the initial rise in concentration and secondary, controlled release of insulin. The trend in the first intercept (Fig. 4A) was related to the difference in dispersivity between water and formulation ($D_i d_i - D_j d_i$). This is equivalent to the induction period (Fig. 3A) noted during in vitro experiments at 92% humidity and 37 °C. The larger the size of the first intercept (c_i, where $i = 1$), the earlier insulin is lost from the formulation and hence its relationship to the in vitro induction period. The controlled phase of insulin release is shown in Fig. 4B (m_i, where $i = 2$) and suggests the balance between energy loss ($D_i d_i - D_j d_i$) and water solubility ($D_j d_i + P_j p_i + H_j h_i + I$) are the governing properties. This is consistent with loss of insulin by erosion of the amorphous surface to reveal a new surface, which is still in the process of relaxation.

The release of insulin in the lungs of rats can, therefore, be ascribed to a rapid initial loss of relaxation energy, followed by the dissolution of the formulation in water with further loss of energy. Since the aqueous solubility of OEDs is very low, the release mechanism of insulin is consistent with local supersaturation of lung fluid with dissolved formulation, followed by crystallisation of OED. In this respect,

the mechanisms of in vitro crystallisation and in vivo release of insulin are similar.

It was noticeable that the TR153 formulation releases very little insulin in vivo following the initial burst. As release of active has been shown to be related to crystallisation of the OED both in vitro and in vivo, this would indicate that in the lung environment there is insufficient water to cause TR153 to crystallise during the course of the experiment. Therefore, although particles in the lung may be immersed in a mucus layer (Geiser et al., 2000), the environment can be described as being closer to one of high humidity than of dispersion in water.

From this study it was concluded that the release of drugs from OED matrices is governed by their interaction with water. When OED microparticles were immersed in water or exposed to high humidity there was an initial period of energy loss before crystallisation begins. Modelling of OED properties suggests that it is the dispersive interactions between the OEDs and water that controls the energy loss, while the duration of this period depends on the OED and the amount of water present, and ranges from minutes (TR101) to days or weeks (TR155). Following the induction period, crystallisation of the OEDs follow first order Arrhenius behaviour, in which water plays a pseudo catalytic role, and release of active closely follows the degree of crystallisation.

References

Alcock, R., Blair, J.A., O'Mahoney, D.J., Raoof, A., Quirk, A.V., 2002. Modifying the release of leuprolide from spray dried OED microparticles. J. Control. Release 82, 429–440.

Archer, W.L., 1992. Hansen solubility parameters for selected cellulose ether derivatives and their use in the pharmaceutical industry. Drug Dev. Ind. Pharm. 18, 599–616.

Baer, H.H., Abbas, S.A., 1979. Synthesis of *O*-*β*-L-fucopyranosyl-(1 → 3)-*O*-*β*-D-galactopyranosyl-(1 → 4)-D-glucopyranose (3′-*O*-*β*-L-fucopyranosyllactose). Carbohydr. Res. 77, 117–129.

Baer, H.H., Radatus, B., 1984. Preparation of some partially protected, α,α-trehalose-type disaccharides having the D-altro configuration. Carbohydr. Res. 128, 165–174.

Blair, J., Mao, L., Hodgers, E., 2000. Modification of the absorption of cyclosporin using Solidose® technology, In: Dalby, R.N., Byron, P.R., Farr, S.J. (Eds.), Respiratory Drug Delivery VII. Interpharm Press Inc., Buffalo Grove, IL, pp. 481–483.

Blair, J., Coghlan, D., Langner, E., Jansen, M., Askey-Sarvar, A., 2002. Sustained delivery of insulin via the lung using Solidose® technology. In: Dalby, R., Byron, P., Peart, J., Farr, S. (Eds.), Respiratory Drug Delivery VIII, vol. 2. Davis Horwood International, North Carolina, pp. 411–413.

Bredereck, H., 1930. Zur konstitution der trehalose. Chem. Ber. 63B, 959–965.

Cerny, L.C., Stasiw, D.M., Zuk, W., 1981. The logistic curve for the fitting of sigmoidal data. Physiol. Chem. Phys. 13, 221–230.

Cleland, J.L., 1997. Protein delivery from biodegradable microspheres. In: Sanders, L.M., Hendren, R.W. (Eds.), Protein Delivery: Physical Systems. Plenum Press, New York, pp. 1–43.

Ding, X., Wang, W., Kong, F., 1997. Detritylation of mono- and di-saccharide derivatives using ferric chloride hydrate. Carbohydr. Res. 303, 445–448.

Geiser, M., Hof, V.I., Gehr, P., Schurch, S., 2000. Structural and interfacial aspects of particle retention. In: Gehr, P., Heyder, J. (Eds.), Particle–Lung Interactions (Lung Biology in Health and Disease, vol. 143). Marcel Dekker, New York, pp. 297–303.

Gribbon, E.M., Hatley, R.H.M., Gard, T., Blair, J.A., Kampinga, J., Roser, B., 1996. Trehalose and novel hydrophobic sugar glasses in drug stabilisation and delivery. In: Karsa, D.R., Stephenson, R.A. (Eds.), Chemical Aspects of Drug Delivery Systems. RSC, London, pp. 138–145.

Hansen, C.M., Anderson, B.H., 1988. The affinities of organic solvents in biological systems. Am. Ind. Hyg. Assoc. J. 49, 301–308.

Hatley, R.H.M., Blair, J.A., 1999. Stabilisation and delivery of labile materials by amorphous carbohydrates and their derivatives. J. Mol. Catal. B: Enzymatic 7, 11–19.

Higuchi, T., 1963. Mechanism of sustained-action medication: theoretical analysis of rate of release of solid drugs in solid matrices. J. Pharm. Sci. 52, 1145–1149.

MATLAB, v12.1, 2001. The MathWorks Inc., 3 Apple Hill Drive, Natick, MA, 01760-2098.

Official Journal of the European Communities, No L 383 A/2, 1992a. Test Method A.8., Partition Coefficient. The Office for Official Publications of the European Communities, Luxembourg, pp. 63–73.

Official Journal of the European Communities, No L 383 A/2, 1992b. Test Method A.6., Solubility. The Office for Official Publications of the European Communities, Luxembourg, pp. 54–62.

ORIGIN User's Manual, 1995. Version 4.0. MICROCAL Software, Inc., Northampton, MA, p. 301.

Ron, E., Langer, R., 1992. Erodible systems. In: Kydonieus, A. (Ed.), Treatise on Controlled Drug Delivery: Fundamentals, Optimisation, Applications. Marcel Dekker Inc., New York, pp. 199–224.

Roskos, K.V., Maskiewicz, R., 1997. Degradable controlled release systems useful for protein delivery. In: Sanders, L.M., Hendren, R.W. (Eds.), Protein Delivery: Physical Systems. Plenum Press, New York, pp. 45–92.

Ryan, A.M., Langner, E., Davidson, I., Blair, J., Goller, M., 2000. Determination and prediction of key OED physicochemical properties: controlled drug delivery using Solidose® technology. In: Dalby, R.N., Byron, P.R., Farr, S.J. (Eds.), Respiratory Drug Delivery VII. Interpharm Press Inc., Buffalo Grove, IL, pp. 485–486.

Scriven, E.F.V., 1983. Dialkylaminopyridines: super acylation and alkylation catalysts. Chem. Soc. Rev. 12, 129–161.

Webb, P.A., Orr, C., 1997. Analytical Methods in Fine Particle Technology. Micrometrics Instrument Corporation, Norcross, GA, pp. 53–63.

Whistler, R.L., BeMiller, J.N. (Eds.), 1972. Methods in Carbohydrate Chemistry, vol. 6. General Carbohydrate Methods. Wiley.

Zhang, J., Zografi, G., 2000. The relationship between "BET" and "free volume" derived parameters for water absorption into amorphous solids. J. Pharm. Sci. 89, 1063–1072.